Seventh Canadian Masonry Symposium
McMaster University
Hamilton, Ontario
June 4-7, 1995

CEMENT BONDED WOOD PARTICLE BLOCKS FOR DRY-STACKED, SURFACE BONDED WALL SYSTEMS

M. M. Khattab[1], R. G. Drysdale[2] and H. J. Rerup[3]

ABSTRACT

An experimental program was conducted to investigate the structural behaviour of a dry stacked surface bonded Durisol block wall system. The Durisol block is composed of cement bonded wood particles. Included in the tests were fourteen three-course prisms tested under concentric and eccentric compression loads and three eight-course walls tested in bending. The test results confirmed very significant axial compression capacities and very ductile behaviour under shear and flexural loads. The need to develop details for transferring floor loads to the wall system was identified.

---

1 Assistant Professor, Ain-Shams University, Cairo, Egypt, on a leave working as Post-doctor fellow at McMaster University, Hamilton, Ontario, Canada.
2 Professor, Department of Civil Engineering, McMaster University, Hamilton, Ontario, Canada, L8S 4L7
3 President, Durisol Materials Limited, Hamilton, Ontario, Canada, L8P 4M3

6-10

Gazzola, E.A. and Drysdale, R.G. (1989), "Strength and Deformational Properties of Dry-Stacked Surface Bonded Low Density Block Masonry", Proceedings of Fifth Canadian Masonry Symposium, Vancouver, BC, June, pp. 609-618.

Glitza, H. (1991), State-of-the-Art and Tendency of Development of Masonry Without Mortar, Proceedings of the 9th International Brick/Block Masonry Conference, Berlin, Vol. 2, 13-16 October, pp. 1028-1033.

Harris, H.G., Oh, K. and Hamid, A.A. (1992), Development of New Interlocking and Mortarless Block Masonry Units for Efficient Building Systems, Proceedings of the 6th Canadian Masonry Symposium, Saskatoon, 15-17 June, pp. 723-734.

Hatzinikolas, M., Elwi, A.E. and Lee, R. (1986), Structural Behaviour of an Interlocking Masonry Block, Proceedings of the 4th Canadian Masonry Symposium, Fredericton, June, pp. 225-239.

INTRODUCTION

Durisol WF blocks have been in use around the world since 1950. Dry stacked, free-standing, the Durisol blocks act as permanent form work for cast in-place, reinforced concrete, load bearing walls. Buildings up to 25 storeys in height have been constructed.

The basic Durisol material is a composition of carefully graded wood chips which are chemically mineralised and bonded under pressure with Portland cement. Hard Durisol is an open textured product, highly durable, practically non-combustible, thermally insulating, vermin proof and does not rot nor decay. Durisol has a density of 650 Kg/m^3.

Figure 1(a) illustrates a cross-section of the current Durisol wall system. The poured in-place concrete core is the load carrying component. Durisol wall systems of this type have an R value of about 1.4 $m^2\,^0C/W$ which is not sufficient for most exterior wall applications based on today's building codes. Higher R values can be achieved by adding sheet insulation to either the interior or exterior faces of the wall.

A modified Durisol wall system is proposed wherein the structural concrete core is eliminated and reinforced structural surface bonded mortar layers are applied to the outside face of the Durisol blocks as shown in Fig. 1(b). In this essentially composite wall system, the mortar layers are the load carrying elements and the Durisol blocks the structural core. The hollow cores are filled with a poured in-place insulating fill thus increasing the wall's R value to above 5.25 $m^2\,^0C/W$; more in line with current code requirements.

The objectives of this investigation were to determine the axial and lateral load capacities of the proposed Durisol wall system and to identify failure modes. Wall load carrying capacities for structures up to three storeys in height were anticipated and achieved.

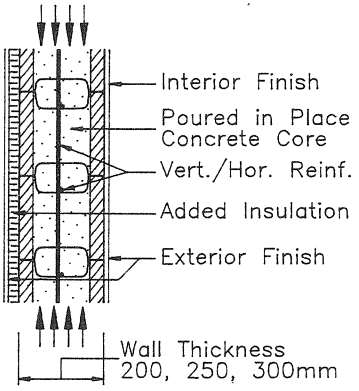

FIG. 1.(a)
Current Durisol
Wall System

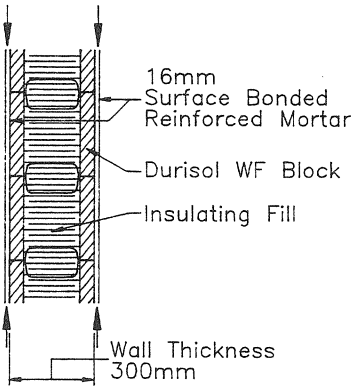

FIG. 1.(b)
Proposed Durisol
Wall System

EXPERIMENTAL PROGRAM

Experimental tests were performed to provide information on the structural performance of surface bonded Durisol walls under axial compression and under bending due to lateral loading. The test program included both three-course prisms tested under eccentric and concentric compression and eight-course walls tested in bending. In addition, individual blocks, coupons of the reinforcement mesh and mortar cubes were tested to serve as control specimens and to define the characteristics of the constituent materials.

Fabrication of Specimens

Both the three and eight-course specimens were built of dry stacked 300 Durisol WF blocks, shown in Fig. 2, stabilized and strengthened with structural mesh-reinforced portland cement mortar parging on the sides as sketched in Fig. 3. To build the specimens, the required number of Durisol blocks were stacked and lengths of mesh, cut to the correct size, were attached to each face of the specimen. The portland cement based mortar coating was then applied on each face. The structural skins created by this mortar parging were applied in two layers of 8 mm making up a total thickness of 16 mm. Wood guides attached along the edges of the specimens helped ensure uniform thickness of parging.

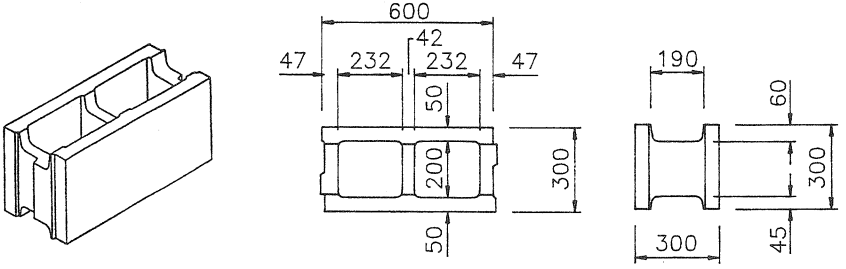

Fig. 2 Standard shape and dimensions of a Durisol block.

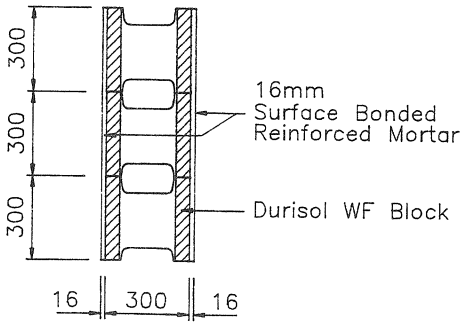

Fig. 3 Vertical section in a typical 3-course prism.

Fourteen three-course prisms were all similarly reinforced with the light wire mesh on both faces. Three eight-course walls were prepared to study the behaviour of the Durisol walls under out-of-plane loads and at the connection with reinforced concrete slabs. Wall WL1 was prepared using light reinforcing mesh, whereas the other two walls (WH1 and WH2) were prepared using a heavy mesh.

Properties of Constituent Materials

The blocks had dimensions of 300x300x600 mm. The standard shape and dimensions of these blocks are shown in Fig. 2. Four Durisol blocks were tested flat wise under uniaxial compression to determine both the compressive strength and the modulus of elasticity. Each block was capped top and bottom with 50.8 mm thick steel plates, using hydrostone capping compound. The stresses were calculated based on a net area of 60000 mm^2. An average compressive strength of 1.11 MPa with a coefficient of variation (C.O.V) of 20.8 % was found. The obtained stress-strain relationships were used to determine the average secant modulus of elasticity as the slope of the secant line from zero to 0.5 of the failure load. The blocks exhibited high compressibility which is reflected by the low average modulus of elasticity of 40.3 MPa. The compressive failures of the blocks were characterised by spalling of wood chips along the mid-heights of the blocks.

Mortar composed of 1.0:0.2:4.1 parts by weight of portland cement, lime and sand was used as parging coats for the specimens. The water/cement ratio of 1.08 was established to satisfy the mason's requirements for workability. This resulted in an average initial flow of 125%. Three 51 mm (2 in.) cubes were prepared as control specimens from each batch. The cubes were air-cured with the specimens and tested a few days after testing the corresponding specimens. The mortar compressive strengths are presented with the test results for corresponding specimens.

Two different types of wire mesh were used in preparing the specimens. The light wire mesh had 1.5 mm diameter wires at 50.8 mm spacing. The horizontal wires had been crimped which tended to hold the mesh about 8 mm off the surface of the blocks. The heavy mesh had 4.78 mm diameter wires at 50.8 mm spacing. Two 500 mm long coupons of the vertical wires were cut randomly from each mesh and tested under uniaxial tension. None of the wires exhibited a clear yield plateau prior to strain hardening. Therefore, the stress corresponding to a strain of 3.5 mm/m was used as the yield stress. This corresponds roughly to the proportional limit for both types of wires. The light and heavy meshes had yield stresses of 282.4 and 631.6 MPa, respectively, and ultimate stresses of 594.8 and 721.5 MPa, respectively.

Test Procedure

According to the loading condition, the three-course prisms can be categorized into three groups. The first group, CP, consisted of five prisms tested under concentric uniaxial compression. The second group, EECP, included six prisms loaded with equal top and bottom eccentricities $e_1=e_2$, whereas the third group, UECP, included three prisms which were loaded with unequal top and bottom eccentricities. The configurations and loading conditions for the three groups are shown in Fig. 4.

Three eight-course walls were tested to study the behaviour of the Durisol walls under out-of-plane loads and at the connection with reinforced concrete slabs. They were tested under a two point concentrated loading arrangement as shown in Fig. 5. Wall WH1 was tested, as shown in Fig. 5(a), having a shear span to depth ratio (a/d) of 2.03. Wall WL1 was tested twice. In the first test, similar to WH1, the wall was tested having a/d equal to 2.03. After

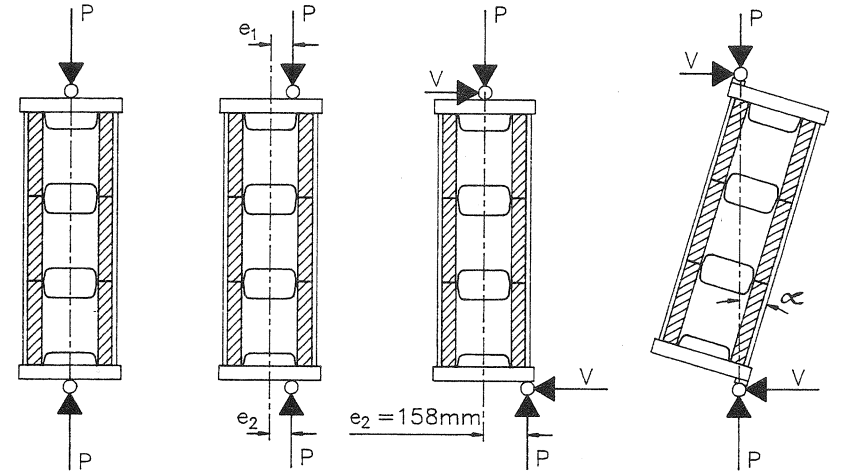

Fig. 4 Loading conditions for three-course prisms.

failure in shear, wall WL1 was tested again to check its flexural capacity. In this test, the loading points were moved closer to the mid span with a/d=2.98 thereby creating a higher ratio of moment to shear. The shear spans, on both ends of the wall, were also bandaged to prevent shear failure.

Wall WH2 was tested twice in order to investigate the effect of the end connection between the wall and the concrete slabs. Concrete end blocks were cast at the two ends of the wall as shown in Fig. 5(b). The concrete in the wall filled the cell space for distance of one block and occupied half the thickness of the space. In the first test, the left end of the wall was supported on the concrete representing a floor slab, as shown in Fig. 5(b). The other end of the wall was supported directly on the reaction roller and the corresponding shear span was bandaged to avoid shear failure. After failure, the wall was tested again, this time being supported, as shown in Fig. 5(c), on the concrete block at the right side. The left shear span was bandaged. In this case, the wall was turned over to create tensile stresses in the webs of the Durisol blocks near the right support.

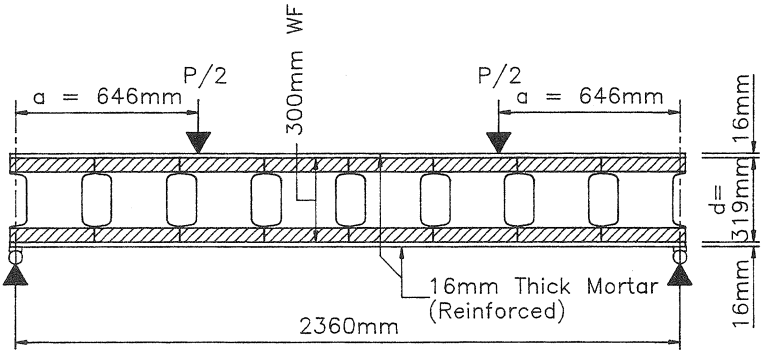

(a) Wall WH1.

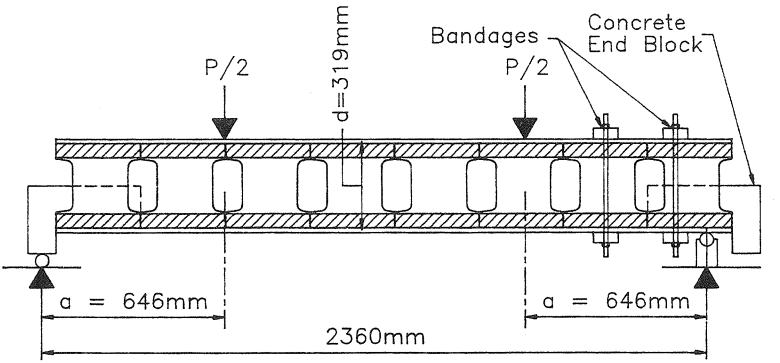

(b) First test of WH2.

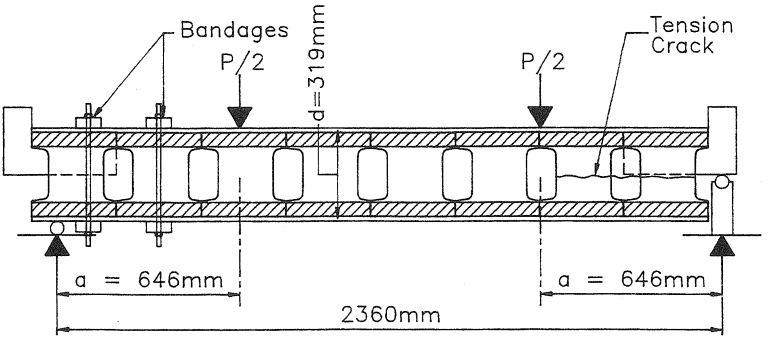

(c) Second test of WH2

Fig. 5 Loading conditions for walls WH1 and WH2.

EXPERIMENTAL TEST RESULTS

Tests of Three-Course Prisms.

Prisms tested under concentric load (Group CP). The five prisms loaded under uniaxial compression were tested to determine the compressive strength as well as the modulus of elasticity of the mortar parged Durisol form of construction. The applied load, along with the strains on the faces of the prisms, were recorded during the test. The measured loads were converted to compressive stresses using only the area of the mortar parging because the modulus of elasticity of the block, as indicated before, was only 40.3 MPa. This value is less than 1/300 of the modulus of elasticity calculated for the prisms tested under uniaxial compression (see Table 1). The mode of failure of the prisms was compression failure of the mortar parge coating characterized by local crushing of part of the mortar coating as shown in Fig. 6(a). The compressive strength and modulus of elasticity results are listed in Table 1.

Table 1 Test results of 3-course prisms tested under uniaxial compression (Group CP).

Prism	Failure Load (kN)	Compressive strength* (MPa)	Modulus of elasticity (MPa)	Mortar compressive strength (MPa)
CP1	170	8.9	9818.5	14.2
CP2	153.7	8	13570.4	14.2
CP3	221.7	11	13390.8	14.2
CP4	209	10.9	--	18.1
CP5	256.6	13.4	--	21.1
Mean	202.2	10.5	12259.9	16.4
C.O.V.	20.3 %	20.3 %	17.3 %	19.2 %

* Strength calculated using the cross-section area of the mortar parging = 19200 mm^2.

Prisms tested under eccentric load with $e_1=e_2$ (Group EECP). Six prisms were tested under eccentric compression having $e_1=e_2$. The first five were tested with $e_1=e_2=158$ mm which placed the load at the centre of one of the mortar parge coatings. The last prism was tested with $e_1=e_2=52.7$ mm which corresponds to 1/6 of the distance between the centres of the mortar parge coatings. The deformations of the two faces of the prisms were recorded at regular increments of the applied loads. Similar to group CP, the stresses were calculated using only the cross-section areas of the mortar coatings. The failures took place, in this case, by spalling of the structural mortar parge coating on the side with the higher compressive stress along with tension cracks in the parge coating on the opposite side in alignment with the joints between the Durisol blocks. The average ultimate compressive load resisted by the prisms in the case of $e_1=e_2=158$ mm was 112.2 kN which was about half the load recorded for the prisms with no eccentricity in group CP. This is to be expected because the load was applied directly over one of the mortar parge coatings and the other could not share the load. The results are summarized in Table 2. For prism EECP6, the statically determined share of the 149.3 kN load on the mortar parge coat nearest the load is 149.3(158+52.7)/316=99.5 kN which is compatible with the capacities of individual parge coats determined from the previous tests.

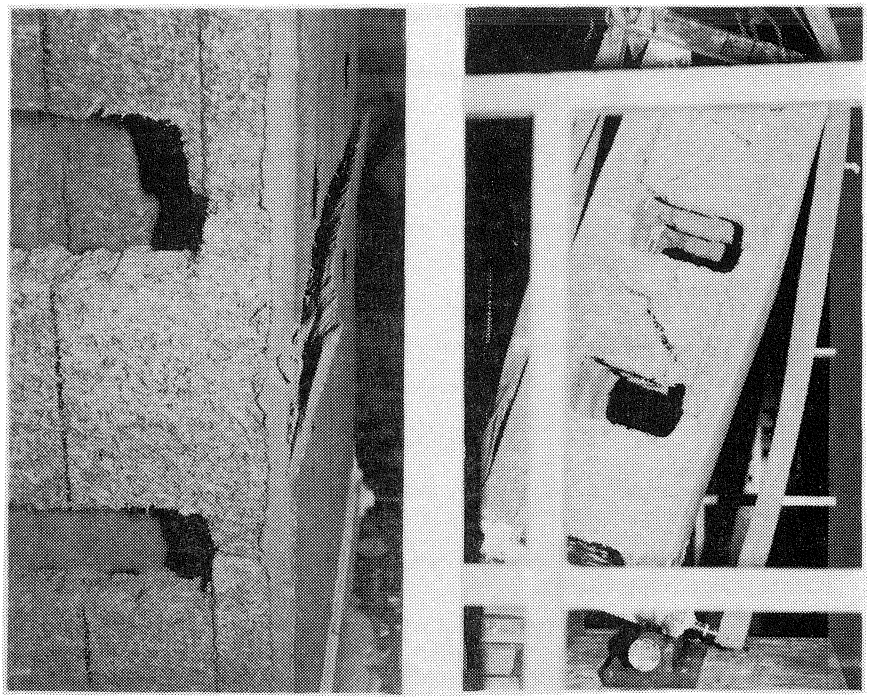

(a) A prism of Group CP after failure. (b) Prism UECP3 after failure.

Fig. 6 Modes of failure of prisms.

Prisms tested under eccentric load with $e_1 \neq e_2$ (Group UECP). Three prisms were tested under compression with e_1 different than e_2. This loading condition was meant to produce shear stresses in the webs of the blocks to define their ultimate shear capacity. (This loading condition represents the case where reversed bending at the ends transfers the axial compression force from one face to the opposite face.) The first prism was loaded so that e_1=0 whereas e_2=158 mm, as shown in Fig. 4(c). The remaining two prisms were tested diagonally, as shown in Fig. 4(d), resulting in e_1=158 mm and e_2=-158 (i.e., e_1/e_2=-1). The failure mode in the three cases was shear failure characterized by diagonal tension cracks in the webs of the blocks as shown in Fig. 6(b). As illustrated in Fig. 4(d) and explained in the footnote of Table 3, lateral shear force V is required for equilibrium of the prisms under the specified loading conditions. It is worth noting that the ultimate axial force P resisted by prism UECP1 was 38.1 kN, which is less than one fifth of the load resisted by prisms with no eccentricity. The ultimate axial loads were much lower with e_1/e_2=-1 in prisms UECP2 and UECP3. The average axial force of 11.55 kN represents a significant limitation where shear failure of the webs of the blocks due to transfer of the force from one face to the other controls the capacity. A summary of the test results is given in Table 3.

Table 2 Test results of 3-course prisms tested with equal top and bottom eccentricities (Group EECP).

Prism[+]	Failure Load (kN)	Ultimate compressive stress[*] (MPa)	Mortar compressive strength (MPa)
EECP1	110	11.5	19.2
EECP2	125.3	13.1	19.2
EECP3	88	9.2	19.2
EECP4	108.3	11.3	18.1
EECP5	129.2	13.5	21.1
EECP6	149.3	10.4	18.1

[+] Prisms EECP1-EECP5 were tested with eccentricity e=158 mm and Prism EECP6 was tested with e=52.7 mm.

* The ultimate compressive stresses were calculated considering the cross-section of the most highly loaded mortar parge coating.

Table 3 Test results of 3-course prisms tested under unequal top and bottom eccentricities (Group UECP).

Prism	e_1, e_2 (mm)	Failure Load P (see Fig. 11) (kN)	Shear force at failure[1] (kN)	Mortar compressive strength (MPa)
UECP1	zero, 158	38.1	5.81	19.2
UECP2	158, -158	11.12	3.95	19.2
UECP3	158, -158	12.02	4.27	19.2

[1] Shear force V in prism UECP1 was determined as; $V=(P \times e_1)/1036$, whereas the shear force in prisms UECP2 and UECP3 were determined as; $V=P (\tan \alpha)$.

[2] The axial force P is the applied load times cos α, as shown in Fig. 4(d).

Tests of Eight-Course Walls

Since each of the walls was tested to serve a particular purpose the results for each wall are discussed separately.

Wall WH1. Cracking took place on the tension side through the mortar coating at the location of the centre joint between the blocks. The cracking moment was 1.07 kN.m as indicated in Table 4. At a load of 6.9 kN, a shear mode of failure took place, characterized by diagonal cracks in the webs of the blocks near the left support. The orientation of the cracks was almost 45° as shown in Fig. 7. At nearly the same load, debonding between the mortar coating and the blocks took place on the other end of the wall. The ultimate shear capacity of the wall at this load was found to be 0.085 MPa, determined as an average shear stress in the webs of

the blocks (Shear stress=shear force/(sum of the widths of the webs x thickness of the block))

Wall WL1. As indicated before, this wall was tested twice. In the first test, (a/d=2.03), the failure took place in shear at an ultimate shear stress of 0.075 MPa. This shear stress is a little lower but fairly close to that of wall WH1. This indicates that the percentage of reinforcement had very little effect on the shear capacity of walls tested under the loading arrangement used.

Because shear failures occurred in the two walls before they were able to achieve their ultimate flexural capacities, the effect of the percentage of reinforcement on flexural strength was not determined. Therefore, to be able to check the flexural capacity of the wall, wall WL1 was tested again. With a/d=2.98 thereby creating a higher ratio of moment to shear. The shear spans, on both ends of the wall, were also bandaged to prevent shear failure. In this test, the wall was able to carry significantly higher load and the failure took place in flexure as the wires failed across the centre joint. The ultimate moment was 3.38 kN.m compared to the maximum moment of 1.92 kN.m reached at shear failure in the first test.

Wall WH2. This wall was tested twice to investigate the effect of the end connection between the wall and the concrete slabs which was simulated by concrete end blocks cast at the two ends of the wall as shown in Fig. 5(b). In the first test, the wall was loaded as shown in Fig. 5(b). The mode of failure in this case was a debonding between the mortar coating and the end block next to the concrete support point. Diagonal cracks appeared also in the webs of the next block (i.e., the second block from the end). The ultimate load was 7.6 kN which resulted in an ultimate shear stress of 0.093 MPa.

The wall was tested again after being turned over, as shown in Fig. 5(c), to create tensile stresses in the webs of the Durisol blocks near the right support. The failure took place at 3.26 kN which is less than half of the failure load obtained from the first test. The failure was characterized by tension splitting cracks along the mid-height of the webs of the blocks, as sketched in Fig. 5(c). The ultimate shear stress in this case was only 0.04 MPa, showing the dramatic effect of the tensile stresses created by the support condition.

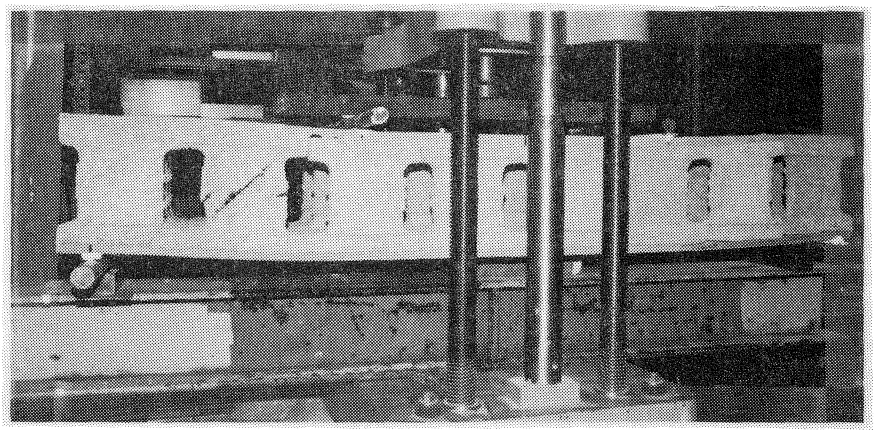

Fig. 7 Wall WH1 after failure.

CONCLUSIONS

The test results confirmed that the proposed Durisol wall system with reinforced surface bonded mortar layers can carry significant axial compression loads. Observed capacities are sufficient for intended three storey buildings. Under out-of-plane flexural loading and unequal eccentric loading the shear strength of the Durisol block webs introduce a limiting factor which needs to be addressed through further testing and modifications. However, out of plane loads, wind for example, are normally relatively low compared to axial loads. The flexible, low modulus, Durisol core allows for significant redistribution of loads through deformation under eccentric loading without brittle failure.

Development of details for transferring floor loads to the wall system is underway. Analytical investigations to define top and bottom of wall rotational restraints is being addressed and will require confirmation through further testing.

ACKNOWLEDGEMENTS

The authors gratefully acknowledge the support provided by the National Research Council, Canada, through the Industrial Research Assistance Program (IRAP), Project No. 026288.